Nonadiabatic dynamics and electronic energy relaxation of Cl(^2P) atoms in solid Ar

A. I. Krylov and R. B. Gerber
Department of Physical Chemistry and The Fritz Haber Research Center, The Hebrew University of Jerusalem, Jerusalem 91904, Israel and Department of Chemistry, University of California Irvine, California 92717

R. D. Coalson
Department of Chemistry, University of Pittsburgh Pittsburgh, Pennsylvania 15260

(Received 4 April 1996; accepted 11 June 1996)

The dynamics of Cl(^2P) atoms in a solid Ar matrix is studied, with emphasis on electronic energy relaxation of excited states, and on p-orbital reorientation effects. The method used follows Tully's approach for nonadiabatic molecular dynamics simulations, which treats the electronic degrees of freedom quantum-mechanically, and the atomic motions classically, allowing for ''hopping'' of the atoms between different potential energy surfaces. We introduce an extended version of this method, to handle ''Berry Phase'' effects due to the doubly degenerate Kramers pairs of states present in this system. The role of both electrostatic and of spin–orbit interactions between different electronic states is incorporated in the treatment. The simulations yield a time scale of 13 ps for the energy relaxation of the highest excited electronic state of Cl(^2P). A time scale of similar magnitude is found for the depolarization of this state. However, the time scale for orbital reorientation at thermal conditions is only 0.7 ps. This is attributed to the fact that at thermal conditions, only the two lowest electronic states are populated. The physical mechanisms of these basic radiationless decay processes are discussed on the basis of the simulations. © *1996 American Institute of Physics.* [S0021-9606(96)01035-5]

I. INTRODUCTION

The understanding of nonadiabatic processes in condensed phases is a challenge of major importance in molecular dynamics. The inherently nonclassical nature of these processes, and the fact that interpretations of the motions involved require more than a single potential energy surface, are among the most interesting, yet complicated, features of the subject. The simulation methods used involved in most cases semiclassical approximations, although also other approaches have been employed.[1–12]

Excited electronic states of guest atoms in rare-gas clusters and in solid matrices have proved a very useful framework, experimentally as well as theoretically, for exploring nonadiabatic dynamics in condensed phases.[13–31] Theoretically, the fact that the interactions involved, including the nonadiabatic coupling between different electronic states, are empirically available for many such systems and are relatively simple in form, is obviously a major advantage.[21–24,27] Experimentally, these systems can conveniently be studied by a variety of spectroscopic techniques.[13–20] Most of the studies explored P-state atoms, where a p-orbital involved gives rise to the degeneracy, or near-degeneracy, of the electronic states causing a breakdown of the adiabatic approximation. The anisotropy of the p-orbital gives rise to polarization behavior that is affected by the dynamics, and adds another interesting aspect to these systems.[30,31]

Most of the theoretical studies of these systems focused on simulations of the electronic absorption spectra, and of related properties.[21–27] Only a few simulations to date have explored the dynamics in time of nonadiabatic processes for atoms in large clusters or in matrices. Thus, nonadiabatic simulations were carried out to explore the dynamics of electronic transitions and of orbital reorientation for F(^2P) atoms in a rare-gas solid.[29,30] Another such study investigated electronic energy relaxation and polarization changes of excited Ba(P) atoms adsorbed at the surface of large Ar clusters, leading to nearly quantitative interpretations of experimental spectroscopic findings for this system.[31] The above studies used a semiclassical ''surface hopping'' method[1,2] for the simulations. Very recently, the dynamics in time of photoexcited $Ba(Ar)_{10}$ and $Ba(Ar)_{20}$ clusters was simulated by a new time-dependent quantum mechanical method, for expected accuracy well beyond the semiclassical approaches.[12] However, all the above simulations considered only nonadiabatic interactions of electrostatic origin. For F(^2P) in rare-gas clusters, the spin–orbit coupling effects were neglected in the studies mentioned above,[29,30] while in the singlet excited state of $Ba(Ar)_n$, such interactions obviously vanish.[31] Yet, in general, spin–orbit interactions are expected to be very important in the dynamics, as they are known to be in spectroscopy, and it is of considerable interest to incorporate these effects in time-dependent nonadiabatic simulations. Spin–orbit interactions can cause significant splittings of electronic levels; they influence greatly orbital orientation and polarization behavior, their symmetry properties differ considerably from those of pure electrostatic systems and interactions, and they greatly change the spectroscopic characterization of many states.

The purpose of the present paper is to study by semiclassical simulations the dynamics in time of nonadiabatic pro-

cesses, in a system where both spin–orbit and electrostatic interactions play a major role. We shall explore electronic energy relaxation and orbital reorientation effects for $Cl(^2P)$ atoms in an Ar matrix. The incorporation of spin–orbit coupling adds complications to the treatment of dynamics, and our objective is to clarify this, as well as throw light on the physical mechanism of nonadiabatic transitions in this case.

The structure of the article is as follows: In Sec. II we describe the system, the electronic states involved, the interaction potentials and the semiclassical simulation method used. In Sec. III the simulation results are presented and discussed. Brief concluding remarks are given in Sec. IV.

II. SYSTEM AND METHODS

The calculations described in this paper, were carried out for a system consisting of a Cl atom in a monosubstitutional site of the *fcc* lattice of solid argon. The simulations treated 256 solid atoms, with periodic boundary conditions at the ends. Evidence from previous simulations for similar systems[29,30] show that the size of the model system used is sufficient for the purpose of the processes studied here.

A. The interaction potentials

The potential energy of the system was described as a sum of contributions from pairwise, spherical Ar–Ar interactions, and of pairwise nonspherical interactions between the $Cl(^2P)$ atom and Ar atoms. Thus, the total interaction potential between all the atoms of the system is given by:

$$\hat{V}=U+\sum_{i>j} u(r_{ij}), \tag{1}$$

where $u(r)$ is the Ar–Ar pair potential, r_{ij} is the distance between the i and the j Ar atoms, and the U represents the interaction between $Cl(^2P)$ and the Ar atoms. The pair potential $u(r)$ between argon atoms was taken from Aziz and Slaman.[32] We used the familiar Diatomics-in-Molecules (DIM) model[33] to describe the anisotropic interaction between the P-state atom and the Ar atoms. In this approach U of Eq. (1) is approximated as a sum of pair interactions between the $Cl(^2P)$ and each Ar atom:

$$U=\sum_{i=1}^{N_a} U_i(r_i,\gamma_i), \tag{2}$$

where r_i is the distance between the Cl and the ith Ar atom, while γ_i is an electronic coordinate representing the angle between the Cl–Ar distance vector $\mathbf{r}_i$, and the orientation of the unpaired p-orbital of the $Cl(^2P)$ atom. We stress that the interaction potential U in this approach, based on electrostatic and empirical considerations, is obviously not a potential in the Born–Oppenheimer sense, since it contains an electronic degree of freedom, the orbital orientation angle. We also note that at this stage, we have not yet included spin–orbit interactions. $U_i(r_i,\gamma_i)$ of Eq. (2) can be expanded in Legendre polynomials, with only two terms contributing in the case of a P-state atom due to symmetry[34]

$$U_i(r_i,\gamma_i)=V_0(r_i)+V_2(r_i)P_2(\cos\ \gamma_i). \tag{3}$$

The interaction potential of Eq. (3) for $Cl(^2P)$-Ar was taken from the work of Aquilanti and co-workers.[35] It is convenient to employ for a system such as considered here a laboratory-fixed coordinate system. In this system, we denote by (θ,ϕ) the orientation angles of the unpaired p-orbital of $Cl(^2P)$. The angle γ_i of Eq. (3) can then be expressed in terms of θ,ϕ and the coordinates for the positions of the Cl atom and the ith argon atom.

To incorporate the spin–orbit interaction effects, we use a simple model that assumes that the spin–orbit splitting is equal to that of an isolated $Cl(^2P)$ atom, and unaffected by the presence of the argon atoms. By this approximation, the spin–orbit coupling operator is given by

$$\hat{V}_{SO}=\Delta\cdot\hat{\mathbf{L}}\cdot\hat{\mathbf{S}}, \tag{4}$$

where $\hat{\mathbf{L}}$ and $\hat{\mathbf{S}}$ are angular momentum and spin operators of the unpaired p-electron of the $Cl(^2P)$. Δ is the spin–orbit splitting of an isolated $Cl(^2P)$ atom (0.1094 eV). Consider now a basis of spin–orbitals $|p_i,\alpha\rangle$, where p_i denotes and uncoupled p spatial orbital, $p_i=\{p_x,p_z,p_y\}$, and α denotes the spin state of the electron. $\mathbf{V}_{SO}$, the matrix which represents $\hat{V}_{SO}$ in this basis, is given by:

$$\mathbf{V}_{SO}=\frac{\Delta}{3}\begin{pmatrix} 0, & 0, & i, & 0, & 1, & 0 \\ 0, & 0, & 0, & 1, & 0, & i \\ -i, & 0, & 0, & 0, & i, & 0 \\ 0, & 1, & 0, & 0, & 0, & -i \\ 1, & 0, & -i, & 0, & 0, & 0 \\ 0, & -i, & 0, & i, & 0, & 0 \end{pmatrix}. \tag{5}$$

Diagonalization of $\mathbf{V}_{SO}$ gives the energy levels of an isolated $Cl(^2P)$ atom. Such an atom has an upper degenerate pair of states $|1/2,1/2\rangle$; $|1/2,-1/2\rangle$ and a lower set of four degenerate states: $|3/2,3/2\rangle$; $|3/2,-3/2\rangle$; $|3/2,1/2\rangle$; $|3/2,-1/2\rangle$. The splitting between the upper states $|j=1/2,\ m_j=\pm1/2\rangle$ and the lower states $|j=3/2,\ m_j=\pm3/2\rangle$, $|j=3/2,\ m_j=\pm1/2\rangle$ equals the spin–orbit splitting parameter Δ.

The adiabatic potential energy surfaces of $Cl(^2P)$ in solid argon are obtained by diagonalizing the operator

$$\hat{W}=\hat{V}+\hat{V}_{SO}, \tag{6}$$

where $\hat{V}$ is the electrostatic interaction among the atoms, given in Eq. (1). There are thus six adiabatic potential energy surfaces, that can be written:

$$W_i(q_1,\ldots,q_N)=\mathrm{Diag}[\langle p_k,\alpha|U+\hat{V}_{SO}|p_l,\alpha'\rangle]+\sum_{m>n} u(r_{mn}), \tag{7}$$

where $q_1,\ldots,q_N$ denote the coordinates of all the atoms in the system, on which the adiabatic potentials depend. The degeneracy of the $W_j(q_1,\ldots,q_N)$ is lower than that of the isolated $Cl(^2P)$ levels, since the electrostatic interactions with the Ar atoms split part of the degenerate states. The degeneracy for given $|m_j|$ is removed by these interactions, while degeneracy of $\{+m_j,-m_j\}$ pairs (Kramers pairs)[36] remains. Indeed, this degeneracy is implied by the Kramers

theorem, which states that there is a twofold degeneracy of systems with a total half-integer spin value that cannot be broken by electrostatic interactions.[36] The six adiabatic surfaces $W_i(q_1,\ldots,q_N)$ of Eq. (7) thus consist of a set of three exactly degenerate pairs of potential functions.

B. The semiclassical nonadiabatic simulation method

The simulation method employed here is based on Tully's ''surface hopping'' approach.[2] Except for the specific aspects necessary for proper treatment of the Kramers degeneracy which are introduced in this paper, the version used here is quite similar to that employed by Krylov *et al.* in recent studies of F(^2P) atoms in solid Kr,[29,30] and of excited Ba(P) atoms adsorbed at the surfaces of large Ar clusters.[31] Different, but closely related semiclassical algorithms were used be Gersonde and Gabriel[37] and by Batista and Coker[38] in simulations of photodissociation and geminate recombinations of molecules in rare gas solids. In fact, several semiclassical methods have been proposed for simulations of nonadiabatic processes,[1–11] and there are no criteria as yet to determine which of these should be best in a given application. Indeed, nonadiabatic transitions in $\mathrm{Ba}(P)(\mathrm{Ar})_n$, for $n=10,20$, were recently studied by a time-dependent quantum mechanical method that is expected to be of greater accuracy than the semiclassical approaches. Comparison in these cases have shown that Tully's surface hopping algorithm gives satisfactory predictions for several properties, but can be in significant deviation from the quantum results in predicting branching ratios for different electronic states for times of the order of 1 ps after excitation. Since the quantum simulation method is not yet feasible for large systems, such as studied here, and since the semiclassical surface hopping method seems adequate at least for many properties of interest we adopt it here.

In the implementation of the surface-hopping method here, we use adiabatic electronic states and the transitions between them to describe the dynamics.[31] Depending on physical considerations, one may choose also other electronic basic states, e.g., the states of the ''bare,'' noninteracting Cl(^2P) atom, and compute transitions between the latter.[29,30] In the present case, the adiabatic electronic states seem a much better basis to employ: The transition between these states, that include already the matrix effect are relatively infrequent, as expected of good ''zero order'' states. Suppose that initially the atoms of the system move on one of the adiabatic potential surfaces $W_i(\mathbf{q})$, $\mathbf{q}=q_1,\ldots,q_N$, defined as in Eq. (7). As long as nonadiabatic transitions do not occur, the atoms are propagated by classical trajectories on that surface. At any point in time, along the trajectory, one can compute the adiabatic potential surfaces $W_j(\mathbf{q})$ (of which there are six in the present case), and the corresponding adiabatic electronic states $\phi_j(\gamma,\mathbf{q})$. This is done ''on the fly'' by diagonalizing the interaction operator $\hat{W}$ of Eq. (6), in the basis of spin–orbitals $|p_i,\alpha\rangle$, discussed in previous subsection. The diagonalization yields uniquely the eigenvalues $W_j(\mathbf{q})$ at each configuration $\mathbf{q}$ of the nuclei. Note, however, that the electronic eigenfunctions $\phi_j(\gamma,\mathbf{q})$ are not uniquely determined in this way. If the $W_j(\mathbf{q})$ are not (exactly) degenerate at $\mathbf{q}$, then $\phi_j(\gamma,\mathbf{q})$ is ambiguous within a $\mathbf{q}$-dependent phase factor $\exp[i\lambda(\mathbf{q})]$, where $\lambda(\mathbf{q})$ is a real-valued function. However, the adiabatic states can be chosen to be real-valued in this case, and the algorithm for calculating the nonadiabatic transitions discussed below is then well-defined.[31,39,40] The situation is more complicated when there is an exact degeneracy, as is the case for the system treated here due to the Kramers state pairs. If $W_1(\mathbf{q}),W_2(\mathbf{q})$ are two degenerate adiabatic potentials, then the corresponding adiabatic wavefunctions are ambiguous within a linear transformation. If $\phi_1(\gamma,\mathbf{q}),\phi_2(\gamma,\mathbf{q})$ are any pair of degenerate, mutually orthogonal electronic eigenstates, then so is any pair of states obtained by

$$\tilde{\phi}_j(\gamma,\mathbf{q})=\sum_{i=1}^{2} a_{ji}(\mathbf{q})\,\phi_i(\gamma,\mathbf{q}), \tag{8}$$

where the $a_{ij}(\mathbf{q})$ correspond to a unitary transformation. For a proper, well-defined calculation of the nonadiabatic transitions, a unique device of the electronic states as a (smooth) function of $\mathbf{q}$ must be made. This is directly related to the topic of Berry Phases.[39] An algorithm that adequately fixes the choice of the (degenerate) electronic eigenfunctions obtained by diagonalization was given by Krylov and Baranov,[40] and is briefly discussed in the next subsection. We assume here that the $\phi_i(\gamma,\mathbf{q})$ are available as unique, analytic functions of $\mathbf{q}$.

We apply now a version of the semiclassical surface-hopping method, closely following Tully.[2] Suppose that initially the system moves on one of the adiabatic potential surfaces $W_j(\mathbf{q})$. As long as nonadiabatic transitions do not occur, the system is propagated by classical molecular dynamics on that surface. At each configuration $\mathbf{q}=\mathbf{q}(t)$, all the adiabatic potential surfaces $W_1(\mathbf{q}),\ldots,W_6(\mathbf{q})$ and the corresponding electronic states $\phi_j(\gamma,\mathbf{q})$ are generated. Since these states are generated ''on the fly'' along a trajectory $\mathbf{q}(t)$, we can write $\phi_j(\gamma,\mathbf{q})\equiv\phi_j(\gamma,t)$ for that trajectory. The electronic degree of freedom is defined in this approach by a wave function $\psi=\psi(\gamma,t)$, that evolves in time according to the Schrödinger equation:

$$i\hbar\,\frac{\partial\psi(\gamma,t)}{\partial t}=[H_0(\gamma)+\hat{W}(\mathbf{q},\gamma)]\psi. \tag{9}$$

$H_0(\gamma)$ is the electronic Hamiltonian associated with the (free) Cl atom, but excluding the spin–orbit coupling. The eigenfunctions of $H_0(\gamma)$ are thus the spin–orbitals $|p_i,\alpha\rangle$. The interaction operation $\hat{W}$, given by Eq. (6), includes the electrostatic interaction $\hat{V}$ and the spin–orbit coupling $\hat{V}_{\mathrm{SO}}$, both of which couple the spin–orbitals $|p_i,\alpha\rangle$. The nuclear motions are described by classical trajectories, so we write $\hat{W}(\gamma,t)\equiv\hat{W}[\gamma,\mathbf{q}(t)]$, a time-dependent interaction acting on the electronic degree of freedom in Eq. (8). We expand the electronic wave function of $\psi(\gamma,\mathbf{q})$ in the adiabatic basis $\phi_j(\gamma,t)$:

$$\psi(\gamma,t)=\sum_{j=1}^{6} C_j(t)\,\phi_j(\gamma,\mathbf{q}). \tag{10}$$

This results in the following equations for the coefficients C_j, given by Tully[2]

$$i\dot{C}_k(t) = -i\sum_j C_j(t)\langle\phi_k|\dot{\phi}_j\rangle + \sum_j C_j(t)W_j[\mathbf{q}(t)]. \tag{11}$$

Using the properties of adiabatic eigenstates, we have for k and j from different Kramers Pairs:

$$\langle\phi_k(\gamma,\mathbf{q})|\nabla_q\phi_j(\gamma,\mathbf{q})\rangle_\gamma = \frac{\langle\phi_k(\gamma,\mathbf{q})|\nabla_q U(\mathbf{q},\gamma)|\phi_j(\gamma,\mathbf{q})\rangle_\gamma}{W_j(\mathbf{q}) - W_k(\mathbf{q})}. \tag{12}$$

In deriving Eq. (11), we used the fact that the spin–orbit coupling in our model is assumed to be independent of the interatomic distances. Using the classical motion of the nuclear coordinates $\mathbf{q}$ we have:

$$\left\langle \phi_k \middle| \frac{\partial\phi_j}{\partial t} \right\rangle = \dot{\mathbf{q}}(t)\langle\phi_k(\gamma,\mathbf{q})|\nabla_q\phi_j(\gamma,\mathbf{q})\rangle_\gamma. \tag{13}$$

Here $U(\mathbf{q},\gamma)$ is defined in Eq. (2), and $\dot{\mathbf{q}}$ is the N-dimensional velocity vector of the nuclei. Eqs. (10) and (11) provide a convenient way for analytical calculation of the time-dependent quantities $\langle\phi_k|\dot{\phi}_j\rangle_\gamma$ which represent the nonadiabatic coupling. These are also computed ''on the fly,'' with the propagation of the trajectory $\mathbf{q}(t)$. Note, that the diagonal derivative matrix elements $\langle\phi_j(\gamma,\mathbf{q})|\nabla_q\phi_j(\gamma,\mathbf{q})\rangle$ are nonzero in the present case since ϕ_j are not real valued. Such diagonal derivative matrix elements are similar to the gauge potentials for nuclear wave functions in Berry's Phase context.[39] It can be shown that in the classical limit in which the Eq. (9) is obtained, the nuclear motion does not depend on the electronic wavefunction phase choice. The arbitrarily chosen phases of ϕ_i define phases of C_i of Eq. (10) by Eq. (11). Also Eq. (12) can not be used to calculate matrix elements between the states that are a Kramers Pair. The analytical expressions for calculation of these matrix elements are developed in Ref. 40. This will be briefly discussed in the next subsection.

The classical propagation of the nuclei, together with Eqs. (10)–(12) for the electronic states and for the nonadiabatic couplings between these states, are the basis of the ''surface hopping'' algorithm. Suppose that initially $C_j(t_0)=1$, $C_k(t_0)=0$ for $k\neq j$. The nuclei are then propagated on the adiabatic surface $W_j(\mathbf{q})$. At each point along the trajectory the six adiabatic potentials and the corresponding eigenstates are constructed, and the nonadiabatic couplings $\langle\phi_k|\dot{\phi}_j\rangle$ are obtained. Equation (10) for the coefficients $C_l(t)$, $l=1,...,6$ are solved numerically, and their variation in time is followed. At sufficiently small time intervals, we test for the possible occurrence of a ''surface hopping'' event. $|C_k|^2$ is compared with a generated random number λ, $0\leqslant\lambda<1$, and on the basis of this stochastic criterion it is decided whether a ''hop'' from surface j to k has taken place or not. For stability of the results it was necessary to test for the possible occurrence of hopping each 50 integration steps. More frequent tests for hopping were found not to change the nonadiabatic transition possibilities. This procedure, used also in Ref. 31 differs from the ''minimum number of hops'' criterion used by Tully,[2] but our tests for this, and other similar systems,[31] suggest that the two algorithms should give very similar results. Once a hopping event has occurred at some $t=t_1$, we reset other coefficients: $C_k(t_1)=1$, $C_l(t_1)=0$ for $l\neq k$. The procedure is then continued with the nuclei being propagated on the surface $W_k(\mathbf{q})$. The initial values for the propagation of the trajectory on the new surface are very similar to those discussed by Tully.[2] Equation (10) for the coefficients is also propagated in time, subject to the reset initial conditions of $t=t_1$. In the above discussion we did not explicitly consider the Kramers pairs, and to do this an obvious modification is required. Suppose $j=1,2$ are Kramers pair of states. These states are always degenerate in this system. There is no ''surface hopping'' between states one and two. The electronic state for this pair is a linear combination of any two eigenstates corresponding to this pair. Since this linear combination is maintained throughout the dynamics and there is no ''hopping'' between the two states, it can be said that the Kramers pairs are treated here in the spirit of the Miller–Meyer approach,[7] rather than by surface hopping. The real dynamics of interest is, of course, that of the transition between the three Kramers pairs of states, which are not degenerate exactly, except at rare time points.

C. Gauge constraints and the construction of electronic adiabatic states

The diagonalization of the electronic Hamiltonian at each nuclear configuration $\mathbf{q}$ independently produces electronic states that are not uniquely defined. Rather, when so obtained their definition is arbitrary within $\mathbf{q}$-dependent coefficients, as expressed by Eq. (8) in the case of a two-fold degeneracy (and by a single phase factor when the states are nondegenerate). On the other hand, the calculation of the nonadiabatic coupling coefficients, given by Eq. (12), depend on the $\mathbf{q}$-variation of the $\phi_j(\gamma,\mathbf{q})$. Thus, the electronic wave function obtained by a typical numerical routine performing the Hamiltonian diagonalization only will result in a ''random'' $\mathbf{q}$-dependence of the $\phi_j(\gamma,\mathbf{q})$, with these functions being in general nondifferentiable in $\mathbf{q}$. We note, that for the system at hand the electronic wave functions cannot be chosen to be real-valued, since the Hamiltonian includes spin–orbit coupling (a similar problem arises when an external magnetic field is present). To fix the $\mathbf{q}$-dependence of the adiabatic electronic wave functions, a *gauge constraint* must be adopted.[40] The theoretical basis for this, and related aspects of the geometric (Berry) phase problem have been discussed in depth by Mead[39] and by other authors. We employ an algorithm for the numerical application of the gauge constraint[40] which is suitable for implementation in the context of the propagation, ''on the fly'' method for obtaining the nonadiabatic couplings used here. The algorithm we use is derived and discussed in detail in Ref. 40, and only a very brief outline is given below.

Let $\phi_j(\gamma,\mathbf{q})$, $j=1,2$, be a pair of degenerate electronic states obtained by diagonalization of the electronic Hamiltonian at the configuration $\mathbf{q}$. As discussed above, the

q-dependence of these states is ''random.'' Our objective is to construct a pair of states $\tilde{\phi}_j(\gamma,\mathbf{q})$, related to the ''randomly generated'' $\phi_j(\gamma,\mathbf{q})$ by the unitary transformation Eq. (8), so that the $\tilde{\phi}_j(\gamma,\mathbf{q})$ be differentiable in **q**. Let $\Phi_j(\gamma,\mathbf{q}_0)$ be a *fixed* pair of states pertaining to a *reference geometry* $\mathbf{q}_0$. We construct the function

$$F(a_{ij})=\sum_{j=1}^{2}|\Phi_j(\gamma,\mathbf{q}_0)-\tilde{\phi}_j(\gamma,\mathbf{q})|^2, \tag{14}$$

and search for the unitary matrix $\mathbf{a}=\{a_{ij}(\mathbf{q})\}$ that minimizes F:

$$F=\min_{a_{ij}}F\{a_{ij}\}. \tag{15}$$

This leads, after considerable algebra, to the following algorithm:[40]

(i) Compute the 2×2 overlap matrix **S** between the reference states Φ_i and the ''random'' states ϕ_j:

$$S_{ij}=\langle\Phi_i|\phi_j\rangle_\gamma, \tag{16}$$

(ii) The overlap matrix S can be decomposed in the form

$$\mathbf{S}=\mathbf{u}\sigma\mathbf{v}^\dagger, \tag{17}$$

where **u**, **v**, σ are 2×2 matrices such that

$$\mathbf{u}^\dagger\mathbf{u}=1,\quad \mathbf{v}^\dagger\cdot\mathbf{v}=1, \tag{18}$$

and σ is a diagonal, positive definite matrix

$$\sigma_{ii}>0 \tag{19}$$

(iii) It can be shown that[40]

$$\mathbf{a}=\mathbf{v}\mathbf{u}^\dagger, \tag{20}$$

where $\mathbf{a}(\mathbf{q})$ is the desired unitary transformation, Eq. (8), from the ''random'' $\phi_j(\gamma,\mathbf{q})$ to the **q**-differentiable $\tilde{\phi}_j(\gamma,\mathbf{q})$. The $\tilde{\phi}_j(\gamma,\mathbf{q})$ are thus readily generated. The values **S**, **u**, $\mathbf{v}^\dagger$ obtained at configuration **q** should be stored for the next step, to obtain $\phi_j(\gamma,\mathbf{q}')$ at $\mathbf{q}+\Delta\mathbf{q}$.

Finally, we discuss briefly the calculation of the matrix elements between Kramers states.[40] We note, that these compliment Eq. (12) of the previous subsection for the derivative couplings between states that are not mutual Kramers Pairs. The derivative matrix elements for the block of degenerate states reads:

$$\langle\phi_i|\frac{\partial}{\partial q_\alpha}|\phi_j\rangle=i\xi_{ij}^\alpha, \tag{21}$$

where α labels the particular Cartesian coordinate, $\alpha\equiv q_\alpha$, and ξ^α is:

$$\begin{aligned}
&\xi^\alpha=\mathbf{u}\tilde{\xi}^\alpha\mathbf{u}^+,\quad \tilde{\xi}_{ij}^\alpha=\frac{\tilde{B}_{ij}^\alpha}{\sigma_i+\sigma_j},\\
&\tilde{B}^\alpha=\mathbf{u}^+B^\alpha\mathbf{u},\quad B^\alpha=i(A^\alpha-A^{\alpha+}),\\
&A_{ij}^\alpha=-\sum_{l\notin K}\frac{S_{il}\langle\tilde{\phi}_l|\partial_\alpha U(\mathbf{q},\gamma)|\tilde{\phi}_j\rangle_\gamma}{W_l(\mathbf{q})-W_i(\mathbf{q})},
\end{aligned} \tag{22}$$

where matrices **u** and σ are given by Eq. (17), matrix **S** is an overlap matrix of Eq. (16) calculated between reference basis set and **q**-differentiable adiabatic states $\tilde{\phi}$, and $\Sigma_{l\notin K}$ means summation over all adiabatic states which are not the ij Kramers pair.

Expressions (22) enables analytical calculation of the diagonal derivative matrix elements and matrix elements between the degenerate states, and indeed for the propagation of the nonadiabatic dynamics algorithm described in Eqs. (9)–(12). The algorithm can readily be extended to any order to degeneracy. Details of the implementation and proofs are given in Ref. 40.

III. RESULTS AND DISCUSSION

We carried out simulations for two types of conditions. One set of calculations corresponded to thermal equilibrium conditions, for the electronic as well as the nuclear degrees of freedom. Also for this thermal equilibrium case we studied processes such as (nonadiabatic) electronic energy relaxation rates and time scales for p-orbital reorientation. These calculations describe essentially the decay of induced perturbations to the equilibrium in the linear response approximation. However, at the temperature of the simulations ($T=17$ K), only the lowest two pairs of adiabatic states are populated. Thus, electronic energy relaxation that takes place in fluctuations is between nearly spaced levels (the average splitting between the lowest pairs of adiabatic states is about 32 cm^{-1}). In the second set of calculations, we assume preparation of the highest pair of adiabatic states. The initial state is taken as a linear combination of two Kramers states with random weights. This is modeled by vertical excitation of the system from its initial thermal state of 17 K. The momentum and positions of the atomic nuclei do not change in this promotion, and the excitation energy used was 0.11 eV. The decay of this state can be viewed as a typical radiationless relaxation process, and the nonadiabatic simulations were used to compute its detailed mechanism, as well as the time scale involved.

A. Simulations for thermal initial conditions

1. Equilibrium populations

Figure 1 shows the populations of adiabatic states computed from simulation at $T=17$ K. The calculation is done only after, by tests, equilibrium has set in. Only the two lowest Kramers pairs of adiabatic states are populated significantly at the temperature used.

The average relative population of the higher pair of states is 4%. This is in some variance with an estimate of 7% which is obtained from Boltzmann factors based on an average splitting of 32 cm^{-1}. This splitting is indicated in Fig. 3 (cf. the higher energy doublet peaks) which is discussed in more detail below. The half-width of the splitting distribution is rather large, 28 cm^{-1}. This leads to variations of the splitting, and consequently to variations in the relative Boltzmann factor for the two states of about 6%. Thus the equilibrium estimation agrees with the result of the dynamics calculations shown in Fig. 1 to within statistical error. Such good agreement between the populations calculated within surface-hopping model and the thermal ones means that the

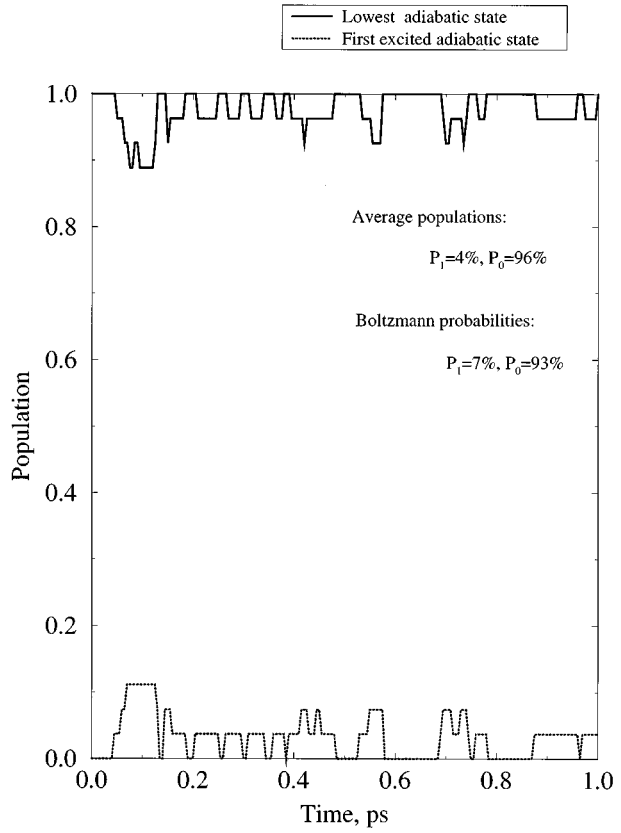

FIG. 1. The populations of the lowest and the first excited adiabatic states. Each state is a degenerate Kramers Pair. The simulations are for equilibrium conditions at $T=17$ K.

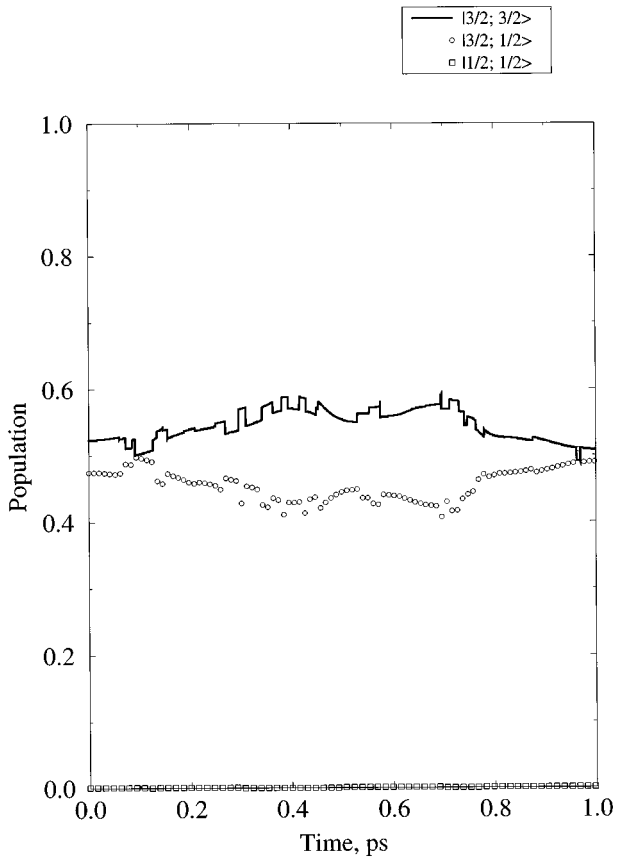

FIG. 2. Populations of bare states $|jm_j\rangle$ of the Cl atom in solid Ar at thermal equilibrium ($T=17$ K). The $|1/2;\pm 1/2\rangle$ population is nearly zero on the scale the plot, as close inspection of the baseline confirms.

criterion for hopping we use is qualitatively good. It is of interest to analyze the populations of the bare states $|jm_j\rangle$ of the isolated Cl atom in the simulated equilibrium ensemble. These populations were obtained by projection of the computed adiabatic electronic states of $Cl(^2P)$ in Ar on the $|jm_j\rangle$ basis functions. The ''bare state'' populations reflect the mixing between bare states due to the electrostatic interaction with the matrix, and therefore, provide a measure of the relative importance of spin–orbit and of electrostatic interactions between the electronic states. The results are shown in Fig. 2.

The $|1/2;\pm 1/2\rangle$ states almost do not couple with the $|3/2;\pm 3/2\rangle$, $|3/2;\pm 1/2\rangle$ states (the mixing coefficient is 0.1%). This means the first excited pair of adiabatic states is essentially pure $|1/2;\pm 1/2\rangle$. The $|3/2;\pm 3/2\rangle$ and $|3/2;\pm 1/2\rangle$ states are mixed with almost equal weights. The dominance of spin–orbit over electrostatic interactions in determining the character of the electronic states is obvious from these results.

2. Spectroscopy

Figure 3 shows the excitation spectrum for isolated Cl atoms in solid Ar. These transitions are forbidden to first order, so direct absorption is bound to be extremely weak. The first peak corresponds to the excitation from the lowest adiabatic to the first excited pair of adiabatic states. As mentioned above, the mean splitting between the two pairs of states is about 32 cm^{-1}. The higher energy doublet corresponds to excitation into the highest adiabatic state, which is almost pure $|1/2;\pm 1/2\rangle$ of the bare Cl atom. The doublet structure is due to excitations from the first excited adiabatic state into the highest $|1/2;\pm 1/2\rangle$ level, in addition to the excitations from the ground electronic state.

3. Orbital reorientation dynamics

To characterize the change in electronic states corresponding to fluctuations from equilibrium and their decay, it was useful to compute certain correlation functions. We thus, computed the autocorrelation function for orbital reorientation $\langle|\mathbf{L}(t)\cdot\mathbf{L}(0)|\rangle$, where $\mathbf{L}(t)$ is the direction of the axis along which the electronic density is maximal. We also computed the autocorrelation function $|\langle\phi(t)\phi(0)\rangle|$, which gives the overlap between the electronic wave function at time t and the initial wave function. The correlation functions were computed after equilibration has set in for both electronic and nuclear degrees of freedom, and with due averaging. Thus in calculating a correlation function $\langle A(t)A(0)\rangle$, we computed $\langle A(t)A(t_0)\rangle$, with averaging also over t_0. The correlation functions $\langle|\mathbf{L}(t)\mathbf{L}(0)|\rangle$, $|\langle\phi(t)|\phi(0)\rangle|$ and $\mathrm{Re}\langle\phi(t)\phi(0)\rangle$ are shown in Fig. 4.

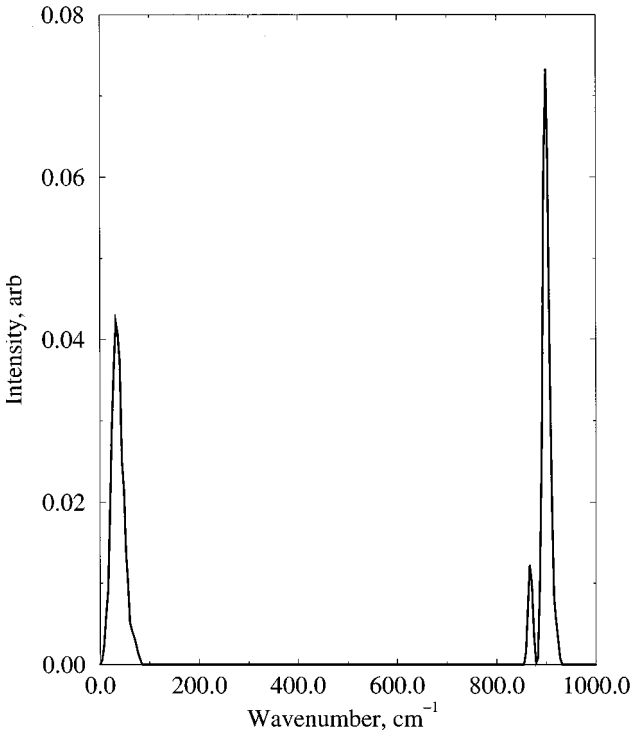

FIG. 3. Electronic excitation spectrum of Cl in solid Ar at 17 K.

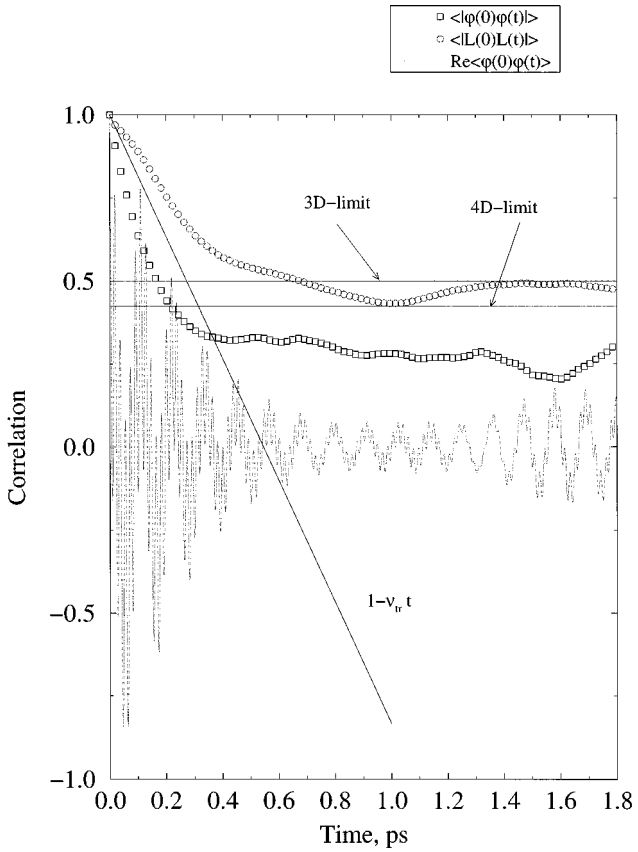

FIG. 4. Electronic correlation functions of thermal fluctuations for Cl in solid Ar at 17 K. The correlation functions shown are $\langle|\mathbf{L}(t)\cdot\mathbf{L}(0)|\rangle$, the orbital orientation correlation; $|\langle\phi(t)|\phi(0)\rangle|$—the correlation function for electronic functions; $\mathrm{Re}\langle\phi(t)|\phi(0)\rangle$, the real part of the electronic correlation function. Statistical limits are discussed in the text.

Neither the orbital orientation correlation function, nor the wave function autocorrelation functions show oscillations. $|\langle\phi(t)\phi(0)\rangle|$ shows an exponential initial decay, $e^{-t/\tau}$, with $\tau=0.28$ ps. The orbital orientation correlation function $\langle|\mathbf{L}(t)\cdot\mathbf{L}(0)|\rangle$ decays initially with a decay time of 0.7 ps. The overlap of the wave function with the initial state decays faster than the orbital orientation because it includes also initial spin decay. The short time behavior is compared in Fig. 4 with a simple model, assuming linear decay in time, with the assumption that the decay is proportional to the mean frequency of nonadiabatic transitions. In previous simulations,[29,30] using the bare $|p_i\rangle$ states of an atom as a basis, rather than the adiabatic states as done here, that model did fairly well at estimating the short-time behavior of $\langle|\mathbf{L}(t)\cdot\mathbf{L}(0)|\rangle$. In the present calculations the decay of the $\langle|\mathbf{L}(t)\cdot\mathbf{L}(0)|\rangle$ correlation function is slower than that given by $1-\nu^{*}t$ (ν-average frequency of nonadiabatic transitions) because the adiabatic states can change their direction in space without making a transition to another adiabatic state. This is not the case with bare states such as $|p_i\rangle$ (used in the study for F in Kr in Ref. 30). Basically, the difference between $\langle|\mathbf{L}(t)\cdot\mathbf{L}(0)|\rangle$ and $1-\nu^{*}t$ shows that much of the orbital reorientation is taking place adiabatically. The classical statistical limit was calculated for the correlation function as the average value of the scalar product $\mathbf{L}(t)\cdot\mathbf{L}(0)$, where the direction of unit vector L is randomly oriented in 3-D space:

$$\langle|\mathbf{L}(t\rightarrow\infty)\cdot\mathbf{L}(0)|\rangle=\frac{1}{4\pi}\int_0^{2\pi}\int_0^{\pi}|\cos\theta|\sin\theta d\theta d\phi=0.5. \tag{23}$$

This limit does not describe correctly the long time behavior of the actual correlation function, because it ignores the role of the spin in the relaxation. A simple quantum statistical limit assumes equal asymptotic population of the four lowest bare states. This, of course, is approximate only but includes both spatial and spin degrees of freedom. This limit was calculated as the average value of the $|\mathbf{L}(t)\cdot\mathbf{L}(0)|$, where the direction of unit vector L is randomly oriented in 4-D space. As it is shown in Fig. 4, 4-D-limit overestimates depolarization of $\mathbf{L}(t)$. It is because the role of the spin is not exactly equivalent to that of a spatial degree of freedom. The long-time behavior of the $|\mathbf{L}(t)\cdot\mathbf{L}(0)|$ can be described as oscillations between 3-D and 4-D limits.

The correlation function $\mathrm{Re}\langle\phi(t)\phi(0)\rangle$ exhibits high frequency oscillations. The Fourier transform of this correlation function is shown in Fig. 5, and includes two frequencies, $\omega_1=47$ cm^{-1} and $\omega_2=291$ cm^{-1}. The frequency ω_2 corresponds to the phase oscillations of the electronic wave function, and equals $E/\hbar$, where E is the average energy of the lowest adiabatic state. This, of course, is the oscillation of the wave function $\phi(t)=\phi(0)e^{-iEt/\hbar}$, when the time-dependence of the Hamiltonian in Eq. (9) can be neglected. The lower frequency $\omega_1=47$ cm^{-1} is close to the average energy splitting between two lowest excited states (32

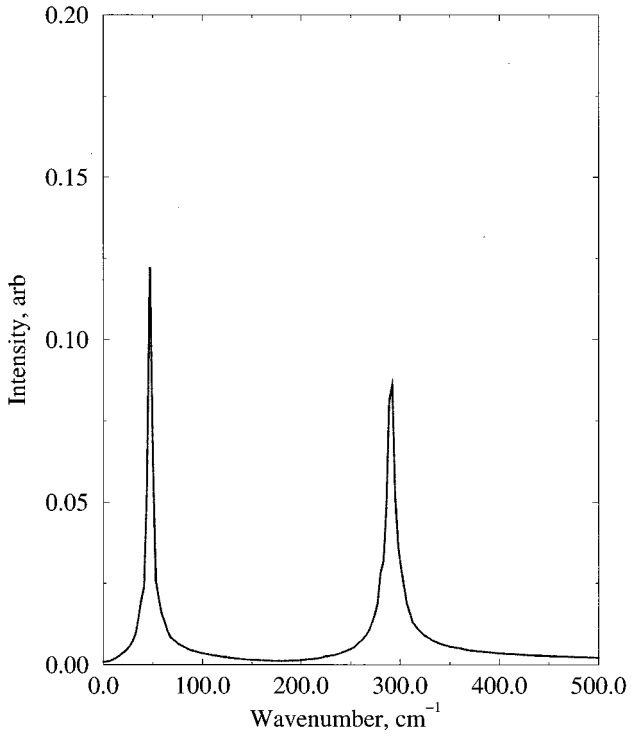

FIG. 5. The Fourier transform of $\mathrm{Re}\langle\phi(t)|\phi(0)\rangle$, the real part of the correlation function of the electronic wave function.

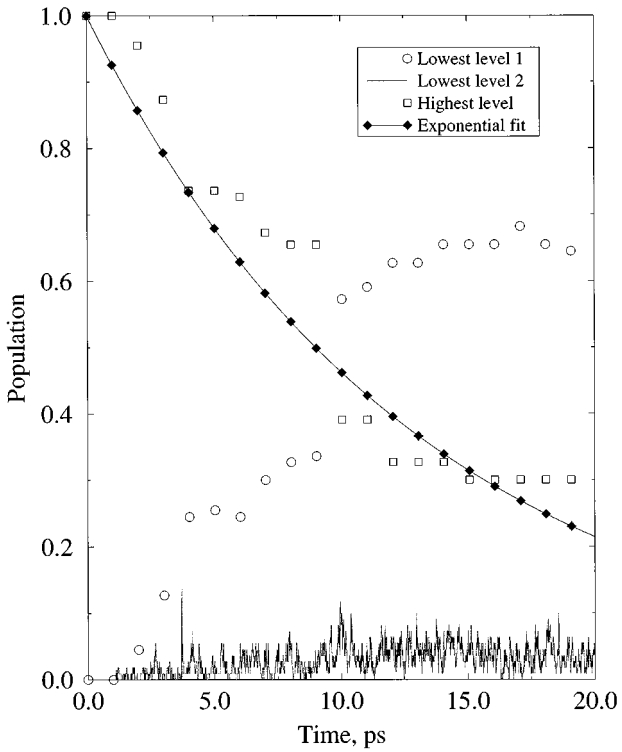

FIG. 6. Relaxation in time of the highest adiabatic level of Cl in Ar at 15 K. Only the highest level was populated at $t=0$. Each population shown is for an adiabatic level corresponding to a Kramers pair of states. Lowest level 1 is a state with the lowest energy. Lowest level 2 is the first excited adiabatic state.

cm^{-1}). Other frequencies that may be relevant, such as the frequency of nonadiabatic transitions, do not show up in the frequency spectrum of Fig. 5, perhaps because their amplitude is small, or due to the large width around $\omega_1=47\ \mathrm{cm}^{-1}$. We conclude this part by a summary of the main results: (i) Both the orbital orientation correlation function and the electronic wave function correlation function decays on the subpicosecond time scale. The correlation function of the orbital orientation decay more slowly than that of the wave function, since the relaxation of the spin variable contributes directly to the latter. Thus, the wave functions can change without an appreciable change in the direction of electron density. (ii) The orbital reorientation relaxation takes place to a large extent (although not only) adiabatically. (iii) The frequency of nonadiabatic transitions gives too fast an estimate for the decay of $\langle|\mathbf{L}(t)\cdot\mathbf{L}(0)|\rangle$: There are many nonadiabatic transitions that do not change the orbital orientation. It should be of great interest to pursue measurements of orbital orientation dynamics, which for systems of the type discussed here are in the subpicosecond range, and may be accessible to study with femtosecond probes using polarization techniques to follow the orbital reorientation.

B. Relaxation of the highest excited state

1. Decay of the excited-state population

Figure 6 shows the population in time of the three adiabatic Kramers pairs of state.

It is assumed that at $t=0$, the system was excited by short pulse of negligible duration to the highest adiabatic level. That level corresponds to an excellent approximation to the pair $|1/2;\ \pm 1/2\rangle$ of bare Cl states. The decay can be fitted to an exponential, with a decay time of $\tau=13$ ps, shown in the figure. Note, that over the time scale of the calculation the population of the first excited adiabatic state (lowest level 2) remains low (almost 6% of the ground-state population). This differs from the equilibrium ratio (4% of the ground-state population), but it must be kept in mind that the system is hotter than the initial temperature due to relaxation. The near-equilibrium seen between the receiving adiabatic levels is expected, since population relaxation from the first excited states to the (degenerate) ground state is much faster than the decay from the higher excited state. This does not reflect on the relaxation mechanism: Analysis of the calculations shows that there is no preference between the lower states (lowest state 1 and lowest state 2, Fig. 6) in the nonadiabatic relaxation from the highest pair of states. The relaxation initially goes almost equally to both the two pairs of states involved because energy spacing between two lowest pairs of states ($32\ \mathrm{cm}^{-1}$) is small compared to the energy gap between highest pair of states and lowest states manifold ($800\ \mathrm{cm}^{-1}$). Later on, population from lowest state 2 relaxes to the lowest state 1 (state of the lowest energy) due to nonadiabatic transitions. This result seems very reasonable, since the energy spacing between the two lower levels is very small, and also because the nonadiabatic interactions involved due, of course, to the electrostatic potentials with the Ar atoms are very similar in magnitude for all the states.

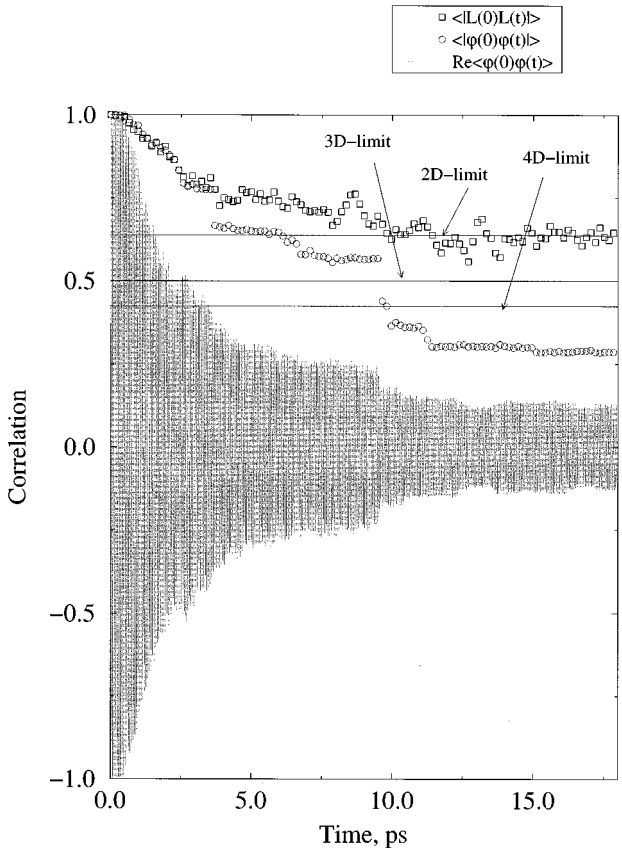

FIG. 7. Correlation functions for the decay of the initially prepared highest adiabatic level of Cl in Ar. The correlation functions shown are $\langle|\mathbf{L}(t)\cdot\mathbf{L}(0)|\rangle$, the orbital orientation correlation; $|\langle\phi(t)\phi(0)\rangle|$—the electronic wave function correlation; and $\mathrm{Re}\{\langle\phi(t)|\phi(0)\rangle\}$.

2. Dynamics of orbital reorientation

As for the case of thermal fluctuations, we found it useful to examine the orbital orientation dynamics in the higher excited adiabatic level through correlation functions.

Figure 7 shows $|\langle\mathbf{L}(t)\cdot\mathbf{L}(0)\rangle|$, the correlation function for orbital reorientation; $|\langle\phi(t)\phi(0)\rangle|$ the correlation function for the wave function magnitudes; and $\mathrm{Re}\langle\phi(t)|\phi(0)\rangle$. Note, the initial level in the simulations is a mixture of the two highest Kramers states with random weights. The time scale for orbital reorientation is of the same order as the excited-state population decay time, and much larger than the orbital reorientation time for thermal fluctuations (in which the two lower adiabatic levels only are involved). The reason for the slow depolarization is simply that no states are available for affecting efficient transitions. The excited level consists of two Kramers states, which correspond nearly exactly to the ''bare atom'' $|1/2;\pm1/2\rangle$ states. Unlike the case of thermal fluctuations there is nearly no state to which coupling can take place and cause depolarization. The only mechanism available involves the inefficient decay to the lower adiabatic levels. Therefore, long-time behavior of $\langle|\mathbf{L}(t)\cdot\mathbf{L}(0)|\rangle$ is described fairly well by 2-D-limit (the 2-D-analog of 3-D and 4-D limits). The 2-D model is relevant here because most of the population is on the *two* equally populated Kramers states.

IV. CONCLUDING REMARKS

In this article, we used semiclassical ''surface hopping'' molecular dynamics simulations to study nonadiabatic processes for a Cl atom immersed in solid Ar. We explored two types of processes: Nonadiabatic events taking place in thermal conditions, in which case only two low-lying adiabatic levels are involved, and nonadiabatic decay of the highest adiabatic level, when initially excited. We found that in thermal conditions the nonadiabatic relaxation, and the process of orbital reorientation were both very fast, on the subpicosecond time scale. The processes are fast due to the availability of other nearby adiabatic states to which coupling can take place. Interestingly, the decay of orbital orientation is much slower than the frequency of nonadiabatic events. Most nonadiabatic events do not change the direction of the electronic density distribution. Transitions in the spin variable contribute to the electronic wave function decay, but not to the orbital reorientation, defined in terms of the axis of maximal electron density. Population decay of the highest excited state is much slower, and in this case the orbital reorientation time scale is the same as that of the population decay. In this case, no states are available for efficient coupling to the highest Kramers pair of states. Only the inefficient coupling to the low nonadiabatic levels remains.

Molecular dynamics simulations of nonadiabatic processes in condensed phases seem to be effective tools for calculations and for obtaining physical insight. Time-resolved spectroscopic studies, using also polarization techniques, seem very desirable and timely as a counterpart for the theoretical studies.

ACKNOWLEDGMENTS

R.B.G. and A.I.K. thank Professor Ara Apkarian for helpful discussions. We also thank Dr. L. Ya. Baranov for useful comments and help, with regard to the Berry Phase issue. The part of this work done at UC Irvine was supported by a grant from the Chemistry Division of the U.S. National Science Foundation (to R.B.G.). The work at The Hebrew University of Jerusalem was supported by a grant from the Israel Science Foundation. The Fritz Haber Research Center is supported by the Minerva Gesellschaft für die Forschung, Munich, Germany.

[1] J. C. Tully and R. K. Preston, J. Chem. Phys. **55**, 562 (1971).
[2] J. C. Tully, J. Chem. Phys. **93**, 1061 (1990).
[3] A. Warshel, J. Phys. Chem. **86**, 2218 (1982).
[4] P. J. Kuntz, J. Chem. Phys. **95**, 141 (1991).
[5] F. Webster, E. T. Wang, P. J. Rossky, and R. A. Friesner, J. Chem. Phys. **100**, 4835 (1994).
[6] D. F. Coker, J. Chem. Phys. **102**, 496 (1995).
[7] H.-D. Meyer and W. H. Miller, J. Chem. Phys. **70**, 3214 (1979).
[8] G. Stock and W. H. Miller, J. Chem. Phys. **99**, 1545 (1993).
[9] R. D. Coalson, D. G. Evans, and A. Nitzan, J. Chem. Phys. **101**, 436 (1994).
[10] R. D. Coalson, J. Phys. Chem. **100**, 7896 (1996).
[11] D. E. Makarov and N. Makri, Phys. Rev. A**48**, 3626 (1993).
[12] P. Jungwirth and R. B. Gerber, J. Chem. Phys. **104**, 5803 (1996).

[13] B. Schilling, M.-A. Gaveau, O. Sublemontier, J.-M. Mestdagh, J.-P. Visticot, X. Biquard, and J. Berlande, J. Chem. Phys. **101**, 5772 (1994).
[14] J.-P. Visticot, P. de Pujo, J.-M. Mestdagh, A. Lallement, J. Berlande, O. Sublemontier, P. Meynadier, and J. Cuvellier, J. Chem. Phys. **100**, 158 (1994).
[15] S. Martrenchard-Barra, C. Jouvet, C. Lardeux-Dedonder, and D. Solgadi, J. Chem. Phys. **98**, 5281 (1993).
[16] A. Stangassiner, J. Scheuchenpflug, T. Prinz, and V. E. Bondybey, Chem. Phys. **178**, 1 (1993).
[17] D. M. Gruen, S. L. Gaudioso, R. L. McBeth, and J. L. Lerner, J. Chem. Phys. **60**, 89 (1974).
[18] C. M. Weinert, F. Forstmann, H. Abe, R. Grinter, and D. M. Kolb, J. Chem. Phys. **77**, 3392 (1982).
[19] C. M. Weinert, F. Forstmann, R. Grinter, and D. M. Kolb, Chem. Phys. **80**, 95 (1983).
[20] T. Hebert, H. Wiggenhauser, U. Schriever, and D. M. Kolb, J. Chem. Phys. **92**, 1575 (1990).
[21] M. E. Fajardo, P. G. Carrick, and J. W. Kenney III, J. Chem. Phys. **94**, 5812 (1991).
[22] M. E. Fajardo, J. Chem. Phys. **98**, 110 (1993).
[23] L. C. Balling and J. J. Wright, J. Chem. Phys. **79**, 2941 (1983).
[24] W. G. Lawrence and V. A. Apkarian, J. Chem. Phys. **101**, 1820 (1994).
[25] I. Last and T. F. George, J. Chem. Phys. **87**, 1183 (1987).
[26] M. E. Fajardo, J. Chem. Phys. **98**, 119 (1993).
[27] A. A. Buchachenko and N. F. Stepanov, J. Chem. Phys. **104**, 9913 (1996).
[28] B. L. Grigorenko, A. V. Nemukhin, and V. A. Apkarian, J. Chem. Phys. **104**, 5510 (1996).
[29] A. I. Krylov, R. B. Gerber, and V. A. Apkarian, J. Phys. Chem. **189**, 261 (1994).
[30] A. I. Krylov and R. B. Gerber, Chem. Phys. Lett. **2312**, 395 (1994).
[31] A. I. Krylov, R. B. Gerber, M. A. Gaveau, J. M. Mestdagh, B. Schilling, and J. P. Visticot, J. Chem. Phys. **104**, 3651 (1996).
[32] R. A. Aziz and M. J. Slaman, Mol. Phys. **58**, 679 (1986).
[33] F. O. Ellison, J. Am. Chem. Soc. **85**, 3540 (1963).
[34] C. H. Becker, P. Casavecchia, Y. T. Lee, R. E. Olson, and Jr W. A. Lester, J. Chem. Phys. **70**, 5477 (1979).
[35] V. Aquilanti, D. Cappelletti, V. Lorent, E. Luzzatti, and F. Pirani, J. Phys. Chem. **97**, 2063 (1993).
[36] P. H. E. Meier and E. Bauer, *Group Theory* (North-Holland, Amsterdam, 1962), p. 253–257.
[37] I. H. Gersonde and H. Gabriel, J. Chem. Phys. **98**, 2094 (1993).
[38] V. S. Batista and D. F. Coker, J. Chem. Phys. (submitted).
[39] C. A. Mead, Rev. Mod. Phys. **64**, 51 (1992).
[40] A. I. Krylov and L. Ya. Baranov, J. Chem. Phys. (to be published).